Transient Temperature Response Modeling in IAMs: The Effects of Over Simplification on the SCC

Alex L. Marten
U.S. Environmental Protection Agency, Washington

Abstract Integrated Assessment Models (IAMs) couple representations of the natural climate system with models of the global economy to capture interactions that are important for the evaluation of potential climate and energy policies. The U.S. federal government currently uses such models to derive the benefits of carbon mitigation policies through estimates of the social cost of carbon (SCC). To remain tractable these models often utilize highly simplified representations of complex natural, social, and economic systems. This makes IAMs susceptible to oversimplification by failing to capture key features of the underlying system that are important for policy analysis. In this paper we focus on one area in which these models appear to have fallen into such a trap. We consider three prominent IAMs, DICE, FUND, and PAGE, and examine the way in which these models represent the transient temperature response to increases in radiative forcing. We compare the highly simplified temperature response models in these IAMs to two upwelling diffusion energy balance models that better reflect the progressive uptake of heat by the deep ocean. We find that all three IAMs are unable to fully capture important characteristics in the temporal dynamics of temperature response, especially in the case of high equilibrium climate sensitivity. This has serious implications given that these models are often run with distributions for the equilibrium climate sensitivity that contain a positive probability for such states of the world. We find that all else equal the temperature response function utilized in the FUND model results in estimates of the expected SCC that are up to 25% lower than those derived with the more realistic climate models, while the functions used in DICE and PAGE lead to expected SCC estimates up to 40% and 50% higher, respectively.

Correspondence Alex L. Marten**,** National Center for Environmental Economics, U.S. Environmental Protection Agency, Washington, DC 20460, United States; e-mail: marten.alex@epa.gov.

The views expressed in this paper are those of the author and do not necessarily represent those of the U.S. EPA. No Agency endorsement should be inferred.

1 Introduction

Integrated Assessment Models (IAMs) couple representations of the natural climate system with models of the global economy to capture interactions that are important for the evaluation of potential climate and energy policies. In this paper we focus on the class of IAMs commonly used to evaluate the social benefits of climate mitigation policies. These models typically link highly simplified representations of the climate system and the economy to estimate the social welfare lost due to climatic change as a result of anthropogenic greenhouse gas emissions (GHGs). In many cases the level of simplification has been driven by a need to ensure that the "model is empirically tractable" (Nordhaus and Boyer, 2000). Despite the potential dangers associated with the over simplification of highly complex natural, social, and economic systems, to date there has been very little rigorous examination of how it effects the policy prescriptions derived using this class of IAMs.

The important work of van Vuuren et al. (2009) and Warren et al. (2010) are the exception and provide a careful examination of the climate modules within this class of IAMs through inter-model comparisons with more complex models, including three-dimensional Atmosphere-Ocean General Circulation Models (AOGCMs). Their findings suggest that the highly simplified climate models within these IAMs produce results within the range of estimates from more complex models, though as noted by the authors, the differences are large enough to have potential policy implications. Their initial finding is certainly understandable considering these highly simplified models are designed and calibrated so that when given central parameter estimates their results match those of more complex climate models (Nordhaus and Boyer, 2000). However, it has become widely accepted that when considering the benefits of GHG mitigation policy, parametric uncertainty (e.g., Morgan and Dowlatabadi, 1996, Hope, 2008) and in particular the positive probability of parameters lying well above their central values (e.g., Newbold and Daigneault, 2009, Weitzman, 2009) is an issue of extreme importance. In response this class of IAMs is commonly run using Monte Carlo simulations to derive the expected benefits, given distributions around crucial but highly uncertain parameters. This naturally begs the question of whether the simplified components of these reduced form models behave reasonably when parameter values are relatively far away from the mode.

One of the most critical and uncertain parameters in these IAMs is the equilibrium climate sensitivity, typically defined as the change in the equilibrium mean global and annual surface temperature, $\Delta T_{2\times}$ [C], that would result from a sustained doubling of atmospheric CO_2 over its pre-industrial level. Estimates of the parameter, whether through empirical studies or AOGCM simulations, are extremely noisy and the distribution tends to be heavily skewed towards the high end (Roe and Baker, 2007, Knutti and Hegerl, 2008). The Intergovernmental Panel on Climate Change (IPCC, 2007) suggests that $\Delta T_{2\times}$ is "likely" between 2 C and 4.5 C, "very unlikely" to be less than 1.5 C, while noting that there remains a positive probability of values above 6 C. Therefore when these IAMs are run under Monte Carlo simulations to derive the expected benefits of climate mitigation policies, there will be draws of the equilibrium climate sensitivity that lie relatively far from the mode.

The simple climate models within this class of IAMs typically use the equilibrium climate sensitivity to define the long-run temperature anomaly within the system given the current level of radiative forcing, and then assume a transient temperature response proportional to the current distance from this long-run equilibrium. This approach is akin to assuming a world covered by a single well mixed ocean layer (Shine et al., 2005). As a result this method for modeling the

temperature response may not capture important features of system's temporal dynamics. For example, the progressive uptake of heat by the deep ocean has important implications for the transient temperature response, particularly at high values of equilibrium climate sensitivity (Baker and Roe, 2009). Therefore, in this paper we proceed with a careful investigation of the transient temperature response functions within this class of IAMs and their ability to adequately capture the temporal dynamics of climate change particularly at high values of the equilibrium climate sensitivity.

We focus specifically on a suite of three prominent IAMs commonly used to estimate the social cost of carbon. These include the Dynamic Integrated model of Climate and the Economy (DICE, Nordhaus (1993), Nordhaus and Boyer (2000)), the Policy Analysis for the Greenhouse Effect (PAGE, Plambeck and Hope (1996), Hope (2006)) model, and the Climate Framework for Uncertainty, Negotiation, and Distribution (FUND, Tol (1997), Narita et al. (2010)). To better understand the simplifications made by the model developers we compare the structure of these IAM's temperature response functions with an upwelling diffusion energy balance model that represents the heat uptake of the deep ocean. We then conduct a series of simulation experiments to consider the impact of these simplifications on the temporal dynamics of temperature response when the equilibrium climate sensitivity is defined by a highly skewed distribution. These experiments are extended to consider the potential impact of the temperature response model on the social cost of carbon (SCC). We find that all else equal the temperature response function in PAGE can lead to estimates of the expected SCC that are 40-50% higher than those derived with more realistic climate models such as the commonly used Model for the Assessment of Greenhouse-gas Induced Climate Change (MAGICC, Wigley and Raper, 1992, Wigley, 2005). The response function included in the DICE model can result in expected SCC estimates 25-40% higher, and the response function in FUND can lead to expected SCC estimates that are 10-25% lower.

To provide additional background Section 2 presents a brief overview of the equilibrium climate sensitivity. The section also introduces the feedback notation used throughout this paper which allows for easier inter-model comparisons. In Section 3 we introduce a simple upwelling diffusion energy balance model to represent the response of global average surface temperature to changes in radiative forcing. This model is not intended to capture all of the complexities of climate system, but instead serves as a method of building intuition behind both the choices of IAM developers and the potential problems of over simplification. Within this framework we then consider the specifics of temperature response in the current versions of three IAMs: DICE, PAGE and FUND. In Section 4 we compare the different models of the temperature response under common scenarios and assumptions about climate sensitivity uncertainty, followed by an analysis of what these differences might mean for estimates of the SCC. Section 5 provides our concluding remarks.

2 Modeling Uncertainty in Climate Sensitivity

The equilibrium climate sensitivity represents the long-run steady-state mean global and annual surface temperature anomaly, $\Delta T_{2\times}$ [C], that would result from a sustained change in radiative forcing, $\Delta Q_{2\times}$ [W/m^2], equivalent to that produced by a sustained doubling of atmospheric CO_2 over its pre-industrial level, such that given a constant λ [C m^2/W],

$$\Delta T_{2\times} = \lambda \Delta Q_{2\times}. \tag{2.1}$$

To provide the reader with intuition as to why the distribution for $\Delta T_{2\times}$ is typically assumed to be highly skewed towards the upper end we briefly discuss this aggregate measure of climate response in terms of uncertainty regarding climate feedbacks following Hansen et al. (1984) and Roe and Baker (2007). Recasting the discussion of equilibrium climate response in these terms will also allow for easier comparison between IAMs by setting aside small model differences regarding assumptions about the radiative forcing associated with a sustained doubling of atmospheric CO_2, $\Delta Q_{2\times}$.

Absent of climate feedbacks, that is assuming a constant albedo and emissivity for the earth, the constant lambda will be equivalent to the reference (or grey-body) climate sensitivity $\lambda_0 = 0.32$ [C m^2/W] as derived from the law of energy conservation and the Stefan-Boltzmann law (Roe and Baker, 2007). In other words, a sustained doubling of CO_2 in the atmosphere would lead to a increase in the temperature of around 1.2 C. However, the albedo and the emissivity will be effected by the rise in temperature resulting from the increased atmospheric stock of GHGs. For example, the increased temperature will allow for an elevated presence of water vapor in the atmosphere, thereby trapping a greater amount of outgoing radiation and leading to a further increase in the temperature. The presence of predominately positive feedback effects such as changes in water vapor, cloud radiative forcing, and the albedo effects of ice melt suggest that on net $\lambda > \lambda_0$ (Mitchell, 1989). As a first order approximation it may be assumed that these feedback effects are linear in the temperature anomaly and independent such that (2.1) can be expanded to represent the change in global equilibrium temperature, $\Delta T_{2\times}$, as

$$\Delta T_{2\times} = \lambda_0 \Delta Q_{2\times} + f \Delta T_{2\times}, \tag{2.2}$$

where f represent the aggregate strength of the feedback effects. From (2.2) it may be seen that

$$\Delta T_{2\times} = \frac{\lambda_0}{1-f} \Delta Q_{2\times}, \tag{2.3}$$

such that $\lambda = \lambda_0/(1-f)$.

Uncertainty around the equilibrium climate sensitivity stems in large part from uncertainty regarding the magnitude of the climate feedbacks (Bony et al., 2006). Roe and Baker (2007) suggest that this set of additively separable feedback effects may be assumed to each have a strength, that when uncertain, is governed by a normal distribution. Therefore the aggregate feedback effect f will also be distributed normally, with mean $\bar{f}$ and standard deviation σ_f. The probability density function for the equilibrium climate sensitivity will then have the form

$$p\left(\Delta T_{2\times}\right) = \phi\left(1 - \frac{\lambda_0 \Delta Q_{2\times}}{\Delta T_{2\times}} \middle| \bar{f}, \sigma_f\right) \frac{\lambda_0 \Delta Q_{2\times}}{\left(\Delta T_{2\times}\right)^2}, \tag{2.4}$$

where $\phi(\cdot)$ is the normal probability density function. Even though the aggregate feedback strength is assumed to be normal, the inverse relationship with $\Delta T_{2\times}$ results in a distribution for the equilibrium climate sensitivity that is heavily skewed towards high values, a feature common in estimates of the parameter's density function (Roe, 2009).[1]

---

[1] We note that an analogous argument for the shape of the equilibrium climate sensitivity distribution can be made based on empirical observations as well (e.g., Armour and Roe, 2011).
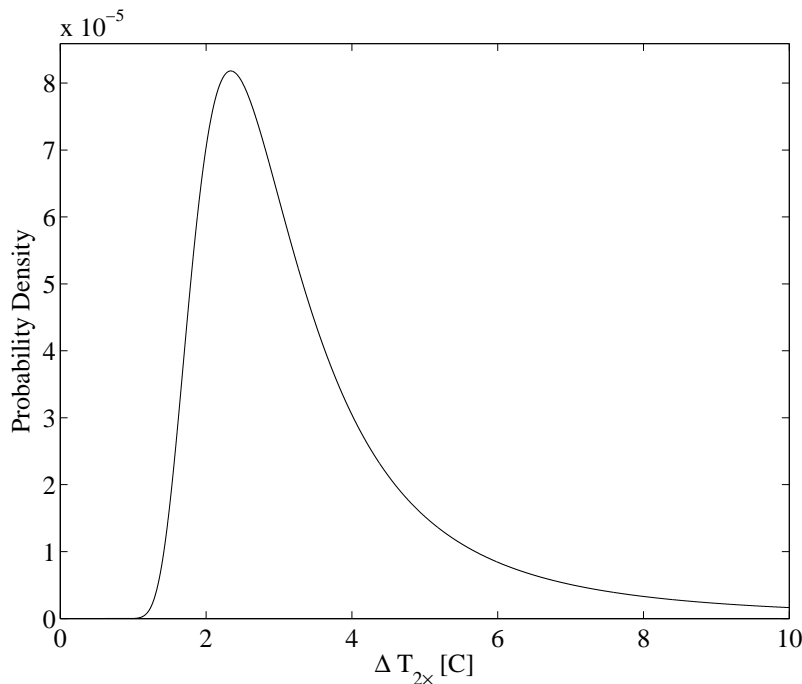
Figure 2.1: Probability Density Function for Equilibrium Climate Sensitivity

The parameters for the distribution are calibrated to match the Intergovernmental Panel on Climate Change summary that $\Delta T_{2\times}$ is "likely" between 2 C and 4.5 C, "most likely" to be around 3 C, while noting that there remains a positive probability of values above 6 C (IPCC, 2007). Throughout this paper we use the specification $\bar{f} = 0.61$ and $\sigma_f = 0.17$, which implies a median equilibrium climate sensitivity of approximately 3 C and a 66% confidence interval of approximately 2 C to 4.5 C. The probability density function of the equilibrium climate sensitivity parameter given this specification is shown in Figure 2.1.

By characterizing the equilibrium climate response to changes in radiative forcing in terms of the constant of proportionality λ instead of $\Delta T_{2\times}$, the parameter of interest no longer depends on the value of radiative forcing associated with a sustained doubling of atmospheric CO_2, $\Delta Q_{2\times}$. This helps provide for a cleaner comparison between model specifications since the three IAMs considered in this paper exhibit slight differences with regards to their assumptions about $\Delta Q_{2\times}$.

3 Modeling the Temperature Response

While the reference climate sensitivity and feedback strength provide a characterization of the long run impacts of a change in radiative forcing on temperature, additional specification is necessary to define the dynamic response of the climate. In this section we present a simple climate system based on the upwelling diffusion energy balance model of Baker and Roe (2009) to represent the response of average global and annual surface temperature to changes in radiative forcing. The model is not intended to capture all of the complexities of the climate system found in larger AOGCMs, but
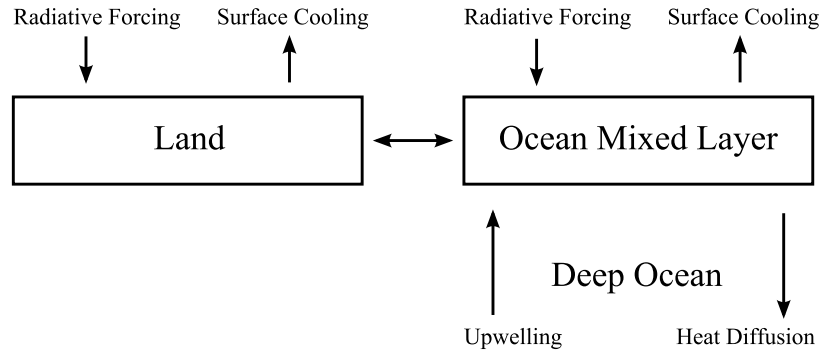
Figure 3.1: Simple Climate Model

is designed to explicitly represent one of the key physical processes that will control the average global surface temperature over long time scales in a tractable manner. It also serves as an ideal framework to discuss the simplifications that led the IAM developers to their specifications of the transient temperature response function in DICE, PAGE, and FUND.

3.1 Simple Upwelling Diffusion Energy Balance Model

The original model of Baker and Roe (2009) assumes a global ocean with a mixed layer that exchanges heat with the atmosphere and a deep ocean. We consider a slight extension to this framework in order to improve the initial dynamics of temperature response by including the presence of land using the same approach as Lindzen and Giannitsis (1998). This results in system, henceforth denoted as UDEB, where a well-mixed upper layer at the ocean surface of depth h [m] exchanges energy with the atmosphere, a deep ocean of depth D [m], and a representation of the earth's land mass. Figure 3.1 provides a diagram depicting this simple system.

The temperature anomaly for the portion of the globe covered by land, as measured by the difference from the initial level and denoted T_t^{Land} [C], is defined by balancing the energy entering the system at time t, as measured by the radiative forcing ΔQ_t [W/m^2], with the layer's thermal radiation and net energy transfer to the ocean's surface layer. Following Lindzen and Giannitsis (1998) the coupling of the land and ocean is defined by a simple linear term that is proportional to the difference in their respective mean temperature anomalies. Therefore given an assumed heat capacity, C_{Land} [W·s/m^2/C], for the land covering a fraction of the globe equal to, A_{Land}, the temperature anomaly T_t^{Land} is defined by the energy balance requirement

$$C_{Land}\frac{dT_t^{Land}}{dt} = \Delta Q_t - \frac{1-f}{\lambda_0}T_t^{Land} - \nu\left(T_t^{Land} - T_t^{Ocean}\right),\tag{3.1}$$

where T_t^{Ocean} [C] denotes the mean temperature anomaly measured as a difference from the initial level for the mixed layer at the ocean's surface.

The mean temperature anomaly for the ocean mixed layer, T_t^{Ocean}, is defined in a similar manner except for the addition of the surface layer's interaction with the deep ocean. In other words, T_t^{Ocean} is defined by balancing the energy entering the system at time t, as measured by the radiative forcing

ΔQ_t [W/m^2], with the mixed-layer's thermal radiation, net energy transfer to the deep ocean, and net energy transfer with the land. The mixed-layer is assumed to have a heat capacity of C_{Ocean} [W·s/m^2/C] and thermal conductivity κ [W/m·C]. The mean temperature of the mixed layer, T_t^{Ocean}, is then defined by the energy balance requirement

$$C_{Ocean}\frac{dT_t^{Ocean}}{dt} = \Delta Q_t - \frac{1-f}{\lambda_0}T_t^{Ocean} + \nu\frac{A_{Land}}{1-A_{Land}}\left(T_t^{Land}-T_t^{Ocean}\right) + \kappa\frac{\partial T_{t,z}^{Ocean}}{\partial z}\bigg|_{z=0}, \quad (3.2)$$

where $T_{t,z}^{Ocean}$ [C] is the temperature anomaly of the deep ocean at time t and depth z. Following Baker and Roe (2009) vertical heat transfer through the deep ocean is defined by an upwelling diffusion process with a vertical diffusivity χ [m^2/s] and an upwelling velocity w [m^2/s], both of which are assumed constant throughout depth and time. The vertical diffusion of temperatures in the deep ocean satisfies the condition

$$\frac{\partial T_{t,z}^{Ocean}}{\partial t} = \chi\frac{\partial^2 T_{t,z}^{Ocean}}{\partial z^2} - w\frac{\partial T_{t,z}^{Ocean}}{\partial z}. \quad (3.3)$$

The mean global and annual surface temperature as measured by a change from the initial level, T_t [C], is defined as the area weighted average of the land and mixed layer temperatures, such that $T_t = A_{Land}T_t^{Land} + (1-A_{Land})T_t^{Ocean}$.

When implementing this model we follow Baker and Roe (2009) in defining the heat capacity of the mixed layer of depth $h = 75$ m as $C_{Ocean} = \rho C_p h$ where $\rho = 10^3$ kg/m^3 is the density of the water and $C_p = 4218$ W·s/kg/C is the heat capacity of the water, in addition to assuming $\kappa = 620$ W/m·C, $w = -1.3 \times 10^{-7}$ m^2/s , and $D = 4,000$ [m]. Following Lindzen and Giannitsis (1998) we assume A_{Land}=0.3, $\nu = 2.83$ W/m^2/C, and that the heat capacity of the land is 30 times smaller per unit area than the mixed layer, such that $C_{Land} = C_{Ocean}/30$. Following MAGICC version 5.3 we set $\chi = 2.3 \times 10^{-4}$ m^2/s (Wigley, 2005). Since there is uncertainty surrounding some of these parameters we note that these specific values are not crucial for the results presented in this paper, and the same conclusions can be made when using other parameter values commonly found in the literature.

We solve the model numerically using an explicit Euler method with 20 intra-annual times steps and spatial steps of 75 m in the deep ocean, along with the assumption of a zero-flux boundary condition at the ocean floor.[2] We also include heat transfer from the surface to the ocean's deepest point to represent bottom water formation bringing surface anomalies to depth following Hoffert et al. (1980) and Baker and Roe (2009). The specifics of the discrete approximation are presented in the Appendix A.

3.2 DICE

The latest version of DICE as described in Nordhaus (2010) models temperature response to changes in radiative forcing in a way that can viewed as a two box simplification of the upwelling

---

[2] The choice of a first order explicit Euler solution was made to reduce the computational burden when implemented within the Monte Carlo simulations of the next section. In comparison with other implicit second order numerical methods such Crank-Nicolson the difference between the solutions is negligible for the purpose of this paper.

diffusion energy balance model discussed in Section 3.1. The system distinguishes between an upper box representing a single global surface layer approximating both the upper ocean mixed layer and land, and a second box representing the deep ocean. The equation identifying the average global and annual temperature anomaly, T_t, in the combined upper ocean/land box may be interpreted as a discrete time version of (3.2) with a time step of one year and a mixed layer depth of $\hat{h} = 360$ [m], such that

$$T_{t+1} = T_t + \frac{s}{\rho C_p \hat{h}} \left[\Delta Q_t - \frac{1 - f_a}{\lambda_0} T_t + \kappa \frac{(T_t - T_t^O)}{D/2} \right], \qquad (3.4)$$

where s is the number of seconds in a year, T_t^O [C] is the mean temperature anomaly for the deep ocean, and κ and D are as defined above. The diffusion of heat through the deep ocean is defined by a simplified representation of (3.3), such that

$$T_{t+1}^O = T_t^O + \delta \left(T_t - T_t^O \right), \qquad (3.5)$$

where the net rate of diffusion $\delta = 0.05$ is said to be chosen to match the results of other climate models (Nordhaus, 2007a). The temperature response model in DICE may therefore be seen as making two major simplifying assumptions relative to the UDEB model in Section 3.1: the land and upper ocean may be represented as a single "well mixed" layer and the deep ocean may be represented as a single well mixed layer also.

3.3 FUND

The integrated assessment model FUND uses an even simpler approach to approximating the temperature response than that of the DICE model. In the FUND model, version 3.5, the earth is modeled as if its covered uniformly by a well mixed single-layer ocean with heat capacity C_{Globe}. There is no explicitly modeled deep ocean and no distinction made between land and sea on the earth's surface. In this case the mean global and annual temperature anomaly is defined by a simplified version of (3.2)

$$C_{Globe} \frac{dT_t}{dt} + \frac{1 - f}{\lambda_0} T_t = \Delta Q_t. \qquad (3.6)$$

A discrete time version of (3.6) with a time step of Δt may be rewritten as

$$T_{t+\Delta t} = T_t + \omega \left(\frac{\lambda_0}{1 - f} \Delta Q_t - T_t \right). \qquad (3.7)$$

This matches the form of the temperature response function currently used in the FUND model, assuming a time step of one year (Narita et al., 2010). Essentially the mean global and annual surface temperature anomaly is modeled as a mean reverting process in which the mean represents the equilibrium temperature that would be reached given a sustained forcing equal to the current level ΔQ_t. The constant ω defines the rate of mean reversion, such that given a sustained change in the level of radiative forcing the half life in terms of reaching the new equilibrium is $\ln(2)/\omega$ years. Equation (3.6) provides a simple definition of ω based on the heat capacity of the system and the

feedback parameter, however using this approach would over estimate the rate at which the system is approaching equilibrium due to absence of vertical heat transfer within the ocean. Recognizing this issue the model developers do not use this direct interpretation instead opting to calibrate the parameter to better match the output of more complex global climate models. In FUND version 3.5 the IAM developers also recognize the dependence of ω on the feedback parameter and model the rate of mean reversion as

$$\omega = \frac{1}{\max\left(\xi_1 + \xi_2 \frac{\lambda_0}{1-f}, 1\right)}, \tag{3.8}$$

where $\xi_1 \sim N\left(-31.90, 0.12^2\right)$ and $\xi_2 \sim N\left(130.91, 0.10^2\right)$, which according to the model documentation (Anthoff and Tol, 2010) is calibrated to match temperature rise for the IS92a scenario of Kattenberg et al. (1996).

3.4 PAGE

In PAGE2002, the latest version of the Policy Analysis for the Greenhouse Effect (PAGE) model, the developers take a similar approach to that used in FUND, where the temperature response is modeled based on the assumption of a single "well mixed" surface layer (Hope, 2006). Therefore PAGE also utilizes the temperature response function in (3.7), with the main difference between the the two models stemming from the calibration of the constant defining the rate of mean reversion.[3] While FUND is careful to include the components of the equilibrium climate sensitivity, PAGE instead opts to model ω as $1 - e^{-1/\kappa}$, where κ is an uncertain parameter from a triangular distribution with a mode of 50, minimum of 25, and maximum of 75 (i.e., PAGE does not include an analog of equation (3.8)).

4 Implications for Temperature Change Projections and the SCC

The different specifications for the temperature response, as described in Sections 3.3-3.4, have significant implications for the projection of future temperature anomalies and in turn the estimates of climate change damages and resulting policy prescriptions. To build an understanding about the general differences of these models in practice we start with a highly controlled experiment in which the climate system is subjected to a sustained radiative forcing equivalent to a doubling of atmospheric CO_2. By eliminating as many moving parts as possible this first exercise provide general insight into the effects of the different modeling choices on projections of future global and annual mean temperature anomalies. We then extend this analysis to consider the case of a given business-as-usual (BAU) socio-economic-emissions scenario typical of the way in which these models are used. Finally we couple the BAU scenario and temperature response models to well cited damage functions from the literature to examine the implications of these inter-model differences for

---

[3] We note that in practice the PAGE models considers spatial variation in the temperature anomaly for eight geographic regions, where the climate response varies across regions due to differences in the level of tropospheric aerosol emissions. However, for the purpose of this paper we ignore this facet of the model as it does not alter our main findings and provides for more compact notation and easier inter-model comparisons.

computing the SCC.

4.1 Temperature Dynamics for a Sustained Forcing

In this first experiment we examine the difference in temperature change projections for the case where the system is subjected to a sustained radiative forcing equivalent to a doubling of atmospheric CO_2 concentrations, $\Delta Q_t \approx 3.7$ W/m^2 $\forall$t (IPCC, 2007). Uncertainty in the feedback factor that determines equilibrium climate sensitivity is represented by $f \sim N\left(0.61, 0.17^2\right)$, as described in Section 2. All other parameters are defined as above, where all model specific uncertain parameters are set to their median so that the following results may be more easily interpreted.[4]

Figure ?? shows the results of a Monte Carlo simulation in which 10,000 projections for the temperature response were computed. The solid line represents the expected path of the temperature anomaly computed over all runs and the shaded area represents the 95% confidence interval for the frequency distribution generated. For comparison the dashed line denotes the path for the median case of $f = 0.6$ which represents an equilibrium climate sensitivity of around 3 C. We begin by considering the difference between the temperature response functions along this path representing a single model run (dashed line). Initially, that is over the first 10-20 years, the temperature response models from the three IAMs project much slower warming than the UDEB model, while suggesting much higher levels of warming in the long term (which we define as over 100 years out). These two timescales represent the initial rapid warming of the thin mixed layer and then the slow adjustment of the deep ocean in the long term. It appears that the highly simplified climate models from the three IAMs are attempting to split the difference between these two time scales. For example, the three functions from the IAMs project a temperature response of around 2.5 C after 100 years and get within a negligible distance of the equilibrium temperature anomaly by the end of 250 years shown. This is a significantly faster rate of warming than suggested by AOGCMs where typically 2/3 of warming occurs within a century and reaching equilibrium requires at least a millennium (Hansen et al., 2008). This timing is more consistent with the projections from the simple upwelling diffusion energy balance model in Figure 4.1a.

The faster than expected temperature response over the time horizon as projected by the models currently used in IAMs is particularly evident when considering the uncertainty surrounding climate feedbacks and in turn the equilibrium climate sensitivity. This is because higher temperature changes at the ocean's surface as a result of stronger climate feedbacks will increase the heat being transferred to the deep ocean, essentially dampening the initial effect of increasing radiative forcing as discussed by Baker and Roe (2009). The result of this effect may be seen in Figure 4.1a where the simple UDEB model projects a change of just under 6 C after 250 years at the 97.5th percentile, which is associated with an equilibrium climate sensitivity of around 11 C. By failing to include an explicit representation of the vertical transfer of heat through the ocean, the temperature response models from the IAMs miss this characteristic. This is most evident by the fact that the temperature response model from PAGE reaches the equilibrium temperature anomaly within 250 years even at the 97.5th percentile, as seen in Figure 4.1c.

---

[4] If model specific uncertain parameters are allowed to vary the primary results due not differ, and any differences in the plots presented are negligible.

(a) UDEB Temperature Response Model

(b) DICE Temperature Response Model

(c) PAGE Temperature Response Model

(d) FUND Temperature Response Model
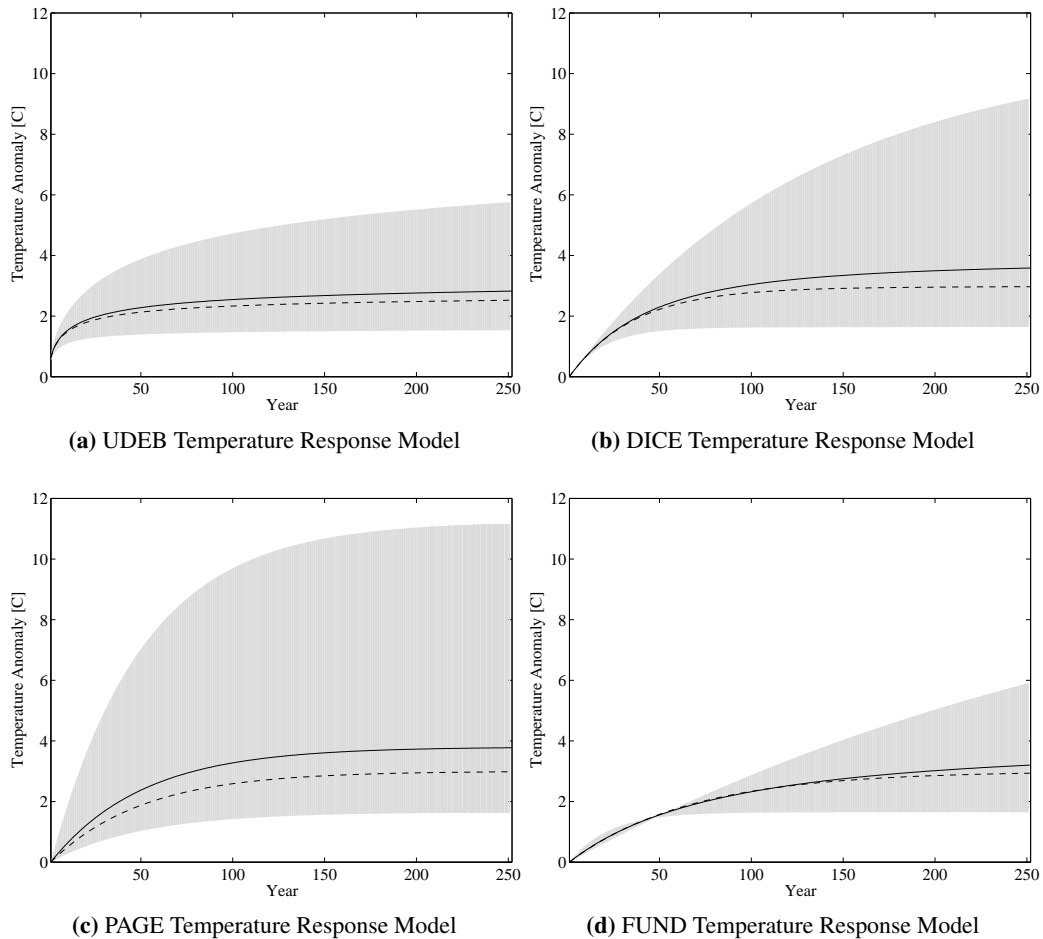
Figure 4.1: Temperature Response to a Sustained Doubling of CO_2

The figures represent the projected temperature response to a sustained radiative forcing of $\Delta Q_t = 3.7$ W/m^2 $\forall t$. The only difference between the runs is the temperature response model and its associated parameters outside of those that define the equilibrium climate sensitivity. All model specific parameters are held constant at their median values and the implied equilibrium climate sensitivity is drawn from the distribution described in the text. The solid line represents the mean temperature response based on a Monte Carlo simulation with 10,000 draws for the climate feedback parameter which determines the equilibrium climate sensitivity and the shaded area represents the 95% confidence interval for the simulation. The dashed line represents a single run at the median implied equilibrium climate sensitivity of 3 C.

The temperature response function in the FUND model does partially incorporate this type of behavior by forcing the rate of mean reversion to depend on the equilibrium climate sensitivity, though in a somewhat ad-hoc fashion. As a result of the inverse relationship specified, at higher values of the equilibrium climate sensitivity the time required to reach equilibrium will be greater. Specifically the rate of mean reversion defined by (3.8) implies that the half life associated with reaching equilibrium is proportional to $1/(a + b\Delta T_{2\times})$, where $\Delta T_{2\times}$ is the equilibrium climate sensitivity. However, as shown by Hansen et al. (1985) the half life is more likely proportional to $1/\Delta T_{2\times}^2$ when considering temperature changes over the next couple of centuries. Therefore the FUND model has difficulty modeling the dynamics of temperature response during the time frame typically considered in policy analysis.

The DICE model with its "two box" representation of the ocean does allow for some transfer of heat to the deep ocean and therefore endogenously captures a portion of this correlation between the rate of atmospheric/upper ocean temperature response and the level of equilibrium climate sensitivity. However, the choice of representing the entire deep ocean as a single well mixed layer prevents the model from capturing this correlation in a robust fashion. At the 97.5^{th} interval the DICE model projects warming over 20% greater than that of the UDEB model.

4.2   Impact of Temperature Response Function on the SCC

The tendency for the temperature response models within these IAMs to initially underestimate the rate of temperature change and then overestimate the expected response in the long-run could have serious implications for their policy prescriptions. We therefore consider the effect this particular modeling choice has on estimates of the SCC, which represents the primary way these IAMs currently enter the policy debate. The SCC denotes the present value of the future damages that would arise from an incremental unit of CO_2 (typically one metric ton) being emitted in a given year. In principle, the SCC summarizes the impacts these additional emissions would have, through their effect on climate change, on all relevant market and non-market sectors, including agriculture, energy production, water availability, human health, coastal communities, biodiversity, and so on. As such, estimates of the SCC play an important role in assessing the benefits of policies that result in reductions of CO_2 emissions.

While each IAM estimates the SCC in a slightly different fashion, the general structure, and the one followed by the recent U.S. Interagency Working Group on the SCC, has a similar set of steps (USG, 2010).

1. Draw uncertain parameters from their defined distributions.

2. Estimate the path of radiative forcing along an exogenous emissions path.

3. Use the temperature response function and radiative forcing path to project the transient temperature change.

4. Compute the welfare loss associated with the temperature change.

5. Perturb CO_2 emissions by one metric tonne in a given year and repeat steps 2-4.

6. Compute the SCC as the net present value of the additional loss of aggregate consumption along the perturbed path.

7. Repeat steps 1-6 within a Monte Carlo simulation to derive the expected SCC.

To capture the change in the SCC that arises from varying assumptions regarding the transient temperature response we fix the components of all steps except for step number 3. Before presenting the results we briefly discuss the assumptions made for each of these steps in turn. When feasible we choose similar assumptions to those used by the U.S. Interagency Working Group on the SCC in order to align this exercise as close as possible with the process currently used to compute the SCC for U.S. federal policy analysis. However, it is important to note that this simple exercise is not attempting to derive specific estimates of the SCC for use in policy analysis and is only intended to demonstrate the relative impact that different specifications of the temperature response model can have on the SCC.

As was done in Section 4.1, the number of moving parts is reduced by setting all uncertain parameters at their medians except for the climate feedback parameter. The distribution for the feedback parameter is defined as $f \sim N(0.61, 0.17^2)$ following Section 2, a specification which is in line with the one used by the U.S. Interagency Working Group on the SCC. To project socio-economic conditions and emissions into the future we follow the U.S. Interagency Working Group on the SCC and use exogenous projections developed as part of the Stanford Energy Modeling Forum study number 22 (EMF-22), specifically we use the reference scenario from the MiniCAM modeling effort (Calvin et al., 2009).[5] Since the EMF-22 scenarios were only computed to 2100 and the SCC is typically computed using longer time horizons we extend the scenario to 2300 closely following the method used by the U.S. Interagency Working Group on the SCC. Specifically, the global population projection is extended by assuming that the growth rate will decline linearly starting in 2100 until it reaches zero in 2300. The growth rate of per capita economic output is assumed to decline linearly from the 2100 level to zero in 2300. The industrial CO_2 emissions projection is extended by assuming that the carbon intensity (CO_2/economic output) growth rate will continue to decline after 2100 at the same rate it averaged between 2090 and 2100. The net CO_2 emissions from land use change is assumed to decline linearly starting in 2100 until it reaches zero in 2200, and all other emissions are assumed to remain constant after 2100. [6]To derive the additional radiative forcing above year 2000 levels along this exogenous emissions scenario we use MAGICC version 5.3 to keep the assumptions regarding atmospheric gas cycles constant across the different temperature response models.[7] To represent the path of historical radiative forcing used to initialize the climate models we consider a basic piecewise linear function where the year 2000 level is determined by a simple energy balance

---

[5] The SCC working group considers four other scenarios from the EMF-22 exercise, however, for readability we focus on a single scenario, noting that the specific scenario chosen is not crucial for our results.

[6] The U.S. Interagency Working Group on the SCC used the assumption that non-CO_2 radiative forcing remained constant after 2100, however they did not specify this assumption in terms of emissions projections. One interpretation would be that in year 2101 all non-CO_2 emissions drop instantaneously to the rate of decay for their atmospheric stocks. Since such a strong discontinuity in emissions at this arbitrary point in the future seems unlikely we instead make the simplifying assumption that all non-CO_2 emissions remain constant after 2100. However, we note that the choice of assumptions regarding post-2100 non-CO_2 emissions does not effect the general results of this paper.

[7] When running MAGICC we use the default parameter values but turn off the carbon cycle feedback effects in order to derive paths of radiative forcing that are independent of the equilibrium climate sensitivity.

equation, the draw of climate feedback strength, and currently observed anomalies following Andreae et al. (2005) and Kiehl (2007). The goal of this approach is to ensure that for each draw of the feedback parameter the path of historical radiative forcing is consistent with current observations. Full details of this approach to initialization are presented in Appendix B.

To standardize the damage function across the temperature response models and maintain the transparency of this experiment we consider two widely cited (and widely divergent) functions from the literature. While the damage functions within each of these IAMs differs considerably, one of the most important characteristic for the purposes of this paper is the shape of the function with respect to mean global and annual temperature anomaly. Therefore we consider two specification of the damage function which differ substantially in their curvature, in order to consider the sensitivity of our results to this feature. In both cases we consider damages, D_t [2007 \$], to be proportional to aggregate consumption, C_t [2007 \$], which is based on economic output as projected by the MiniCAM EMF-22 scenario and a constant savings rate of 22%, a rate that is consistent with the assumptions of the U.S. Interagency Working Group on the SCC. The general structure for the damage function is

$$D_t = \left[1 - \frac{1}{1 - m(T_t)} \right] C_t, \tag{4.1}$$

where $m(T_t)$ is a polynomial with respect to mean global and average temperature anomaly. We consider two specifications for the polynomial, that of the DICE2007 model $m(T_t) = 0.0023888 T_t^2$ as proposed by Nordhaus (2007a) and that of Weitzman (2010) who presents a much more "reactive" damage function, $m(T_t) = 0.0023888 T_t^2 + 0.0000051 T_t^{6.754}$. Figure 4.2 depicts these two specifications. As may be seen, they offer two very different shapes for damages at high temperatures, which is an area of utmost concern when considering the ability of these temperature response models to adequately handle temperature dynamics for high levels of equilibrium climate sensitivity.

Following the steps outlined above we use Monte Carlo simulations to estimate the expected damages over time as a percentage of consumption under each model of the temperature response along the reference scenario. Figure 4.3b and 4.3c present projections of the expected damages for the DICE2007 and Weitzman (2010) damage function specifications, respectively, and Figure 4.3a presents the expected temperature change under the same scenario. For comparison we also include the results using the temperature response model included within MAGICC version 5.3. This represents a more complete upwelling diffusion energy balance model than the one presented in this paper as it accounts for additional complexities in the land/sea interface, includes separate models for the oceans in the northern and southern hemispheres, and allows for variable upwelling rates among other improvements. However, in comparison it may be seen that the simple UDEB model of Section 3.1 provides results which exhibit the same general temporal dynamics as MAGICC. This suggests that for explaining the model differences and understanding the basic intuition behind the dynamics of temperature response, the simpler UDEB framework may be sufficient.

The differences between the projections for the other climate models is as expected based on the experiments of the previous section. The FUND model suggests far slower warming within the next 150-200 years, as compared with the UDEB model and MAGICC. While PAGE and DICE suggest much higher levels of warming since they do not fully account for the uptake of heat by the deep ocean and therefore over estimate the climate response especially at high draws for the equilibrium climate sensitivity. The significant differences in the estimated level of climate damages over this
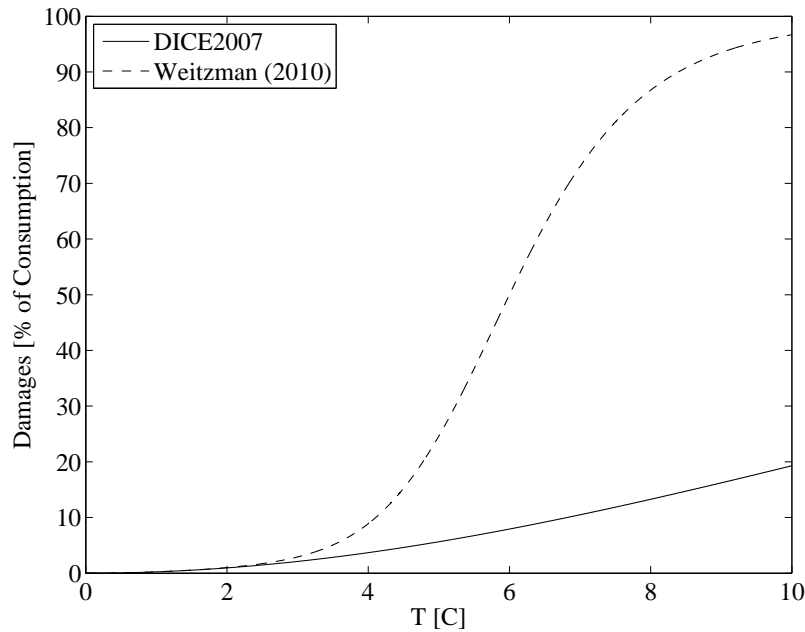
Figure 4.2: Damage Functions

time horizon are then as would be expected, since they will follow the general differences in the projected temperature amplified by the non-linearity of the damage function.

Following the steps outlined above we compute the SCC by considering a second path of radiative forcing derived from a scenario in which an additional ton of CO_2 emissions is released in the year 2010. For each draw of the feedback parameter we compute the projected temperature change and damages along this perturbed path. The SCC for the ith draw is then the net present value of the additional welfare loss due to the extra CO_2 emissions,

$$SCC_i = \sum_{t=0}^{H} \beta_t \left\{ D(T'_{t,i}) - D(T_{t,i}) \right\}, \tag{4.2}$$

where β_t is a discount factor, H is the time horizon (300 years), and T'_t is the projection of the mean global and annual temperature anomaly on the perturbed path.

The temperature response model plays two very important roles in determining the SCC, first it defines the baseline level of the temperature anomaly, which is significant given the non-linearity of the damage function. Second it defines the realized effect of the perturbation on temperature over time. While Figure 4.3 examines the former, Figure 4.4 explicitly considers the second point depicting the projected impact of the perturbation on temperature for the cases of an equilibrium climate sensitivity around 3 C ($f = 0.60$) and 8 C ($f = 0.85$).[8] For the case with an equilibrium

---

[8] The kink in the MAGICC results for the case of $f = 0.85$ is due to the fact that the model incorporates a variable upwelling rate which by default remains constant after the system reaches a temperature anomaly of 8 C. In this case the perturbation causes the model to reach this point in an earlier time period resulting in the non-smooth difference between the two projections of temperature.
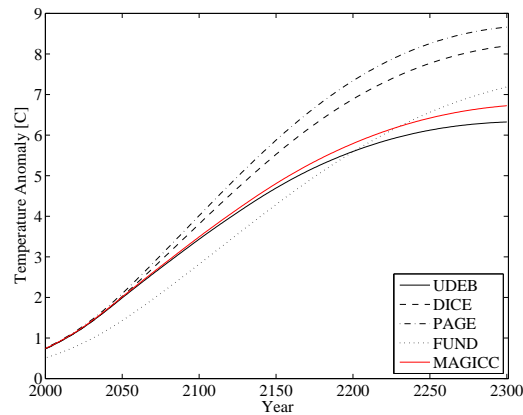
(a) Expected Temperature Change
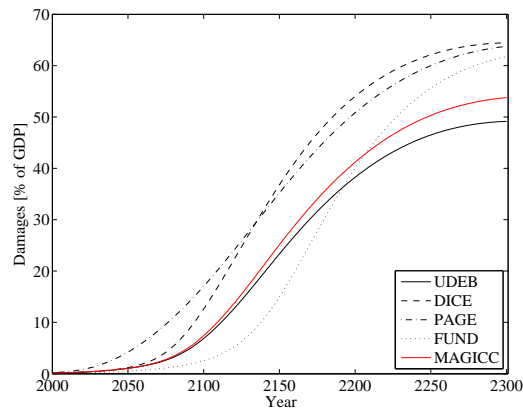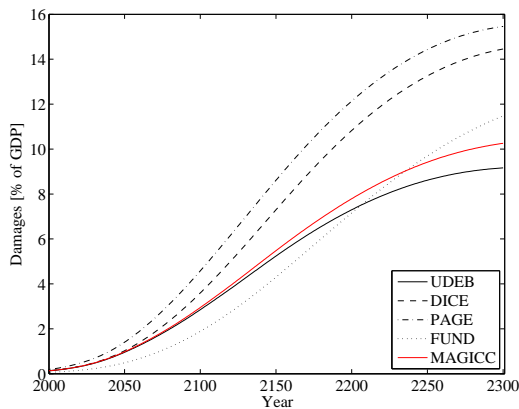
(b) Expected Damage Estimates - DICE2007 Case

(c) Expected Damage Estimates - Weitzman (2010) Case

Figure 4.3: Mean Temperature Change and Damage Estimates

The only difference between the runs is the temperature response model and its associated parameters, outside of those that define the equilibrium climate sensitivity. All model specific parameters are held constant at their median values and the implied equilibrium climate sensitivity is drawn from the distribution described in the text. The lines represent the mean temperature change and damage estimates based on a Monte Carlo simulation with 10,000 draws for the climate feedback parameter which determines the equilibrium climate sensitivity. The baseline radiative forcing scenario is determined by the MiniCAM EMF-22 reference scenario extended to 2300 following the procedure adopted by the U.S. Interagency Working Group on the SCC.

(a) Equilibrium Climate Sensitivity ≈ 3 C   **(b)** Equilibrium Climate Sensitivity ≈ 8 C
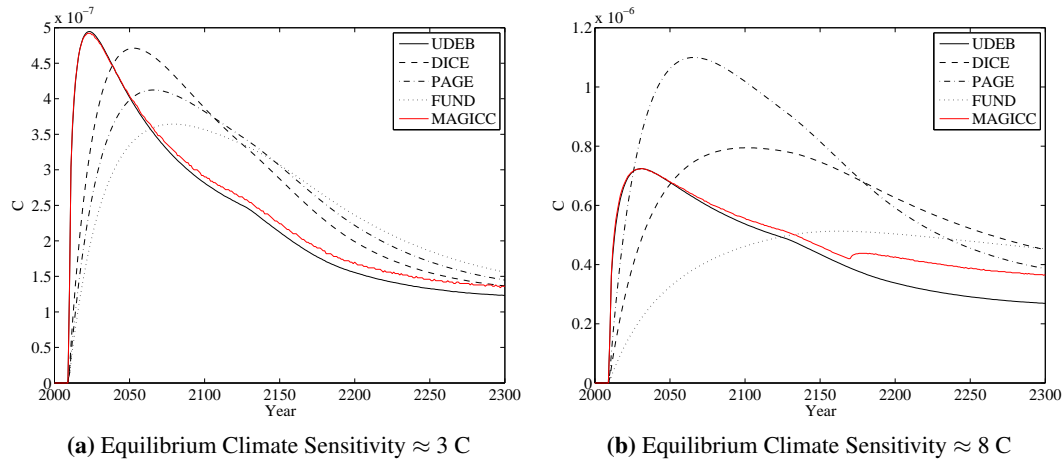
Figure 4.4: Temperature Perturbation From Additional Tonne of CO2 Emissions in 2010

The only difference between the runs is the temperature response model and its associated parameters, outside of those that define the equilibrium climate sensitivity. All model specific parameters are held constant at their median values and the implied equilibrium climate sensitivity is set at approximately 3 C in Figure 4.4a and approximately 8 C in Figure 4.4b. The baseline radiative forcing scenario is determined by the MiniCAM EMF-22 reference scenario extended to 2300 following the procedure adopted by the U.S. Interagency Working Group on the SCC.

climate sensitivity of 3 C the three highly simplified temperature response models in the IAMs require a substantially longer time for the perturbation to reach its peak effect on the temperature relative to the UDEB and MAGICC models. DICE represents the smallest difference in time of around 30 years whereas FUND takes over 50 additional years for the temperature response of the perturbation to reach its peak impact. This difference could have a substantial impact on the SCC given that the stream of marginal damages is discounted. In the case of an equilibrium climate sensitivity significantly higher than the mode, 8 C, the divergence between the models is even more noticeable. In this case the FUND model takes over 130 years longer than the UDEB or MAGICC models to reach the peak impact of the perturbation, which is also significantly lower in magnitude. This suggests that all else equal the temperature response function in the FUND model may lead to significantly lower marginal damage estimates in the case of a high equilibrium climate sensitivity. It may also be seen that in the case of high equilibrium climate sensitivities the PAGE model projects much larger estimates for the magnitude of the perturbation's impact on temperature relative to the UDEB or MAGICC models, which is in line with the results of Section 4.1. This suggests that all else equal the PAGE model will generate significantly higher projections for marginal damages in these cases, potentially leading to substantially higher expected SCC estimates compared to the other temperature response models.

Using the DICE2007 and Weitzman (2010) damage function specifications we compute the expected SCC by taking the average of (4.2) for each of the 10,000 draws of the climate feedback parameter. To test the sensitivity of our results to the specification of the discount rate we consider two specifications. First we use a constant 3% discount rate which corresponds to the central rate considered by the U.S. Interagency Working Group on the SCC and second we compute the SCC

using a Ramsey discounting framework such that

$$\beta_t = \rho + \eta g_t, \tag{4.3}$$

where ρ is the pure rate of time preference, η is the marginal elasticity of substitution, and g_t is the consumption growth rate in period t. The pure rate of time preference discounts future utilities and we set this to zero as has been suggested appropriate for inter-generational problems (e.g., Ramsey, 1928, Stern, 2006). The second component accounts for the fact that individuals in the future will be wealthier and therefore a marginal loss in consumption will have less of an impact on welfare as compared to current populations. For the marginal elasticity of substitution we use $\eta = 1.5$ following Nordhaus (2010). While the constant discount rate approach is the one currently being used by federal policy analysts, the Ramsey approach is relatively more common in the academic literature.

Table **??** presents the mean SCC estimates for the five temperature response models with each discount rate and damage function combination. As would be expected given the previous results the UDEB and MAGICC models provide similar estimates. Also as would be expected from the temperature response to the perturbation depicted in Figure 4.4 the FUND model produces significantly lower estimates. In the case of the constant discount rate, holding all else equal, the FUND temperature response model will produce mean SCC estimates that are around 20-25% lower than those derived using the MAGICC model. The temperature response model from PAGE produces similarly large differences but in the opposite direction. In the constant discount rate case, all else equal, the PAGE temperature response model produced mean SCC estimates that are around 50% higher than estimated using the MAGICC model independent of the damage function specification. The DICE temperature response function produces estimates on the higher side as well, around 25-40% above those derived using MAGICC. The magnitude of these differences suggests that over simplifying the temperature response function to the point of losing important characteristics of the temporal dynamics, could have large implications for how we interpret the policy prescriptions produced by these IAMs.

As one would expect, the choice of discount rate has an effect not only on the SCC itself, but also on the temperature response model's impact on the SCC. In the scenario considered annual economic growth averages around 2.5% over the next 50 years, 2.25% for the following 50 years, and then averages around 1% over the remaining time considered. Even with the pure rate of time preference set to zero the effective discount rate is above 3% for the first 100 years of the simulation, falling to one slightly below 3% after that period. Therefore with these parameter values the Ramsey discounting approach has a slightly higher effective discount rate than the constant 3% case. This is evident in the lower SCC estimates presented in Table **??**. The higher effect discount rate implies that events in the far future, when the simple temperature response functions exhibit the greatest level of divergence, are given less weight in calculating the SCC. As a result the differences between the three highly simplified functions and the MAGICC and UDEB models are sightly lower. However, the differences could still have substantial policy implications, suggesting that the importance of correctly specifying the transient temperature response is independent of the discount rate or damage function being considered.

To better understand the differences in the mean SCC due to changing the temperature response model we consider the full distributions of the SCC derived from the Monte Carlo experiments. Figure 4.5 presents the histograms for the case using the DICE damage function specification and a

**Table 1:** Mean 2010 SCC Comparison Across Temperature Response Models (2007 $)

Discount Rate	Damage Function	Temperature Response Model				
		DICE	PAGE	FUND	UDEB	MAGICC
3%	DICE2007	24	28	15	18	19
	Weitzman (2010)	108	117	59	72	77
Ramsey	DICE2007	21	24	14	16	17
	Weitzman (2010)	90	98	65	67	72

For each row all of the components including radiative forcing paths, implied equilibrium climate sensitivity, damage function, and discount rate are held constant across the temperature response models. The only difference between the columns is the temperature response model that maps changes in radiative forcing to changes in the global annual average temperature anomaly given an implied equilibrium climate sensitivity. Noting that this means the only difference between the PAGE and FUND columns is the treatment of the rate of mean reversion as described in Section 3. The expected SCC values are computed using a Monte Carlo simulation with 10,000 draws for the feedback parameter which defines the equilibrium climate sensitivity, all other parameters are held constant at their median values.

constant 3% discount rate. We have excluded the MAGICC results to save space since they are very similar to those of the UDEB model, as would be expected based on the previous results. Among the the four models the differences in the distributions are substantial, though not unexpected given the results of Section 4.1. The DICE and PAGE temperature response models tend to produce relatively high transient climate responses, particularly at high values of the equilibrium climate sensitivity. As a result their SCC distributions exhibit a greater degree of skewness towards the high end. The PAGE temperature response model leads to a 95th percentile that is nearly 150% higher than that of the UDEB model. On the other hand the FUND temperature response model tends to produce much lower transient temperature response over the next century relative to the upwelling-diffusion energy balance models, UDEB and MAGICC. The result is a much narrower distribution in which the 95th percentile is about 40% lower than that of the UDEB model. The differences exhibited in the upper tails of the distributions has a significant impact on the range of the mean SCC across models ($15-$24) for 2010 compared with the 50th percentile ($14-$19). Since organizations, such as the U.S. Federal Government, utilize the mean to describe the expected benefits of marginal CO_2 emission reductions in policy analysis it is important to ensure that the temperature response model used by these IAMs do not artificially shrink or expand the upper tail of the SCC due to over simplification.

5   Concluding Remarks

For integrated assessment models that estimate the damages associated with anthropogenic greenhouse gas emissions, a key component is the one that translates changes in radiative forcing into changes in surface temperature. In this paper we carefully compare the approaches from three of

(a) UDEB Temperature Response Model

(b) DICE Temperature Response Model

(c) PAGE Temperature Response Model

(d) FUND Temperature Response Model
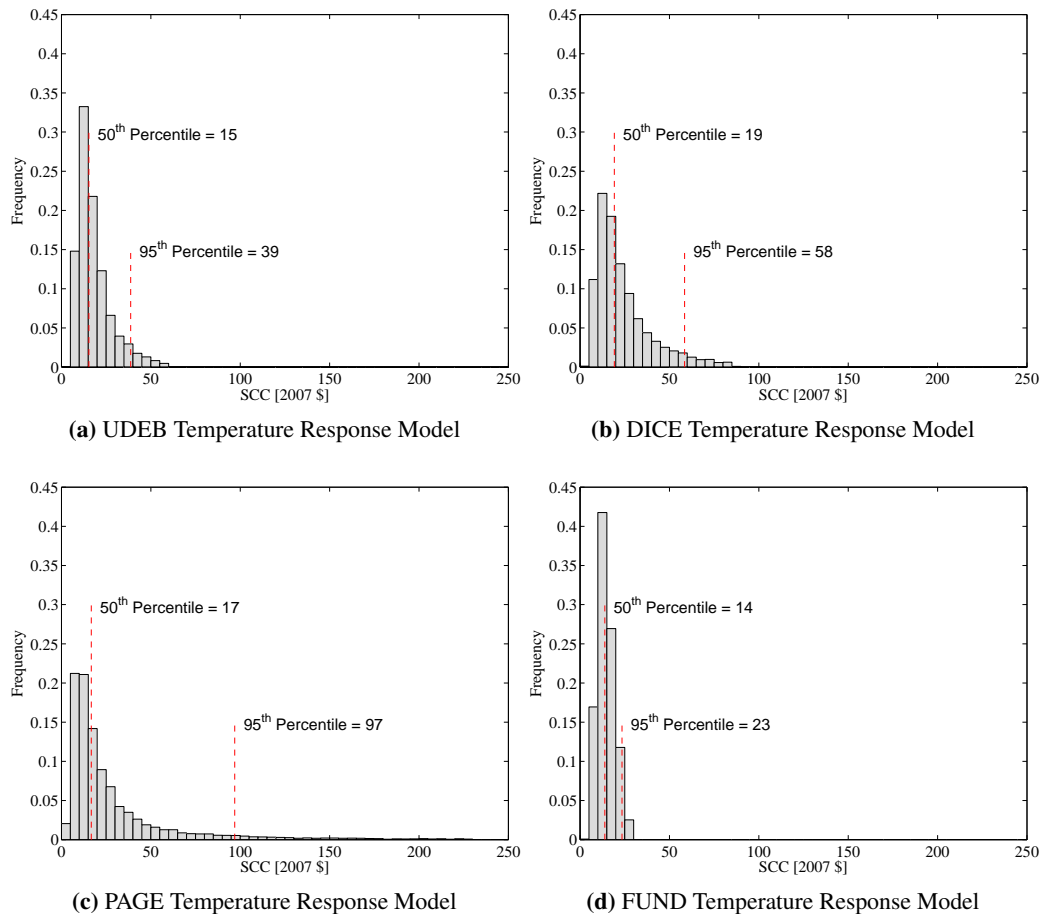
Figure 4.5: SCC Histograms Using DICE Damage Function and Constant 3% Discount Rate

All components of the model including radiative forcing paths, implied equilibrium climate sensitivity, damage function, and discount rate are held constant. The only difference between the panels is the temperature response model that maps changes in radiative forcing to changes in the global annual average temperature anomaly given an implied equilibrium climate sensitivity. The histograms are computed using a Monte Carlo simulation with 10,000 draws for the feedback parameter which defines the equilibrium climate sensitivity, all other parameters are held constant at their median values.

the most prominent IAMs currently being used to value the benefits of carbon mitigation in policy analysis. These models, DICE, PAGE, and FUND, utilize highly simplified functions to approximate the complexities of temperature response dynamics often relying on parameter calibration to make up for not explicitly representing vertical heat diffusion through the ocean. Compared with a more general, but yet still relatively simple, upwelling diffusion energy balance model of climate and ocean dynamics it is clear that the simplified functional forms fail to capture important characteristics of the temperature response dynamics. This is especially true in the case of high equilibrium climate sensitivities, which has strong implications for the suitability of these temperature response models when considering distributions for the parameter that assign a positive probability to such outcomes. We find that using a distribution for the equilibrium climate sensitivity similar to that currently used by the U.S. federal government for policy analysis the FUND model tends to underestimate near term warming, while the PAGE and DICE models tend to substantially overestimate future warming particularly in the case of high climate sensitivities.

We conduct a controlled experiment to study the effect of these modeling assumptions on estimates of the SCC in order to better understand the policy analysis implications of over simplifying the temperature response model. Using a set of commonly cited damage functions from the literature and an exogenous socio-economic-emissions scenario, we compare how switching from a slightly more complete climate model such as MAGICC to one of the highly simplified functions would change the expected SCC. We find that the PAGE temperature response model increases the mean SCC by 40-50% depending on the discount rate, while the DICE model increases the mean estimates by 25-40%, and the FUND model reduces the mean SCC estimates by 10-25%. While these exact results are specific to the setup of this experiment, they are found to be robust to different specifications of the damage function and discount rate. This suggests that the highly simplified temperature response models currently utilized in some IAMs may be inadequate when important issues such as uncertainty regarding the equilibrium climate sensitivity are incorporated into policy analysis. A simple solution for this class of IAMs would be to follow the approach of Marten and Newbold (2011) and rely on existing simple, but more complete, climate models developed by climate scientists, such as MAGICC. The suite of IAMs considered in this paper were originally developed 15-20 years ago and choices with regards to the level of simplification used were in part made to keep the models computationally tractable (Nordhaus and Boyer, 2000). However, over this period computing power has increased by nearly three orders of magnitude (Nordhaus, 2007b) which now allows these IAMs to be coupled with more sophisticated climate models that capture important characteristics of the problem previously lost due to over simplification.

Appendix

A Numerical Approximation for UDEB Climate Model

The explicit first order Euler approximation to the simple climate model presented in (3.1)-(3.3), given the additional condition of bottom water formation bringing surface anomalies to depth may

be represented as

$$T_t^{Land} = T_{t-1}^{Land} + \frac{\Delta t}{C_{Land}} \left[\Delta Q_t - \frac{1-f}{\lambda_0} T_{t-1}^{Land} - \nu \left(T_{t-1}^{Land} - T_{t-1,0}^{Ocean} \right) \right], \tag{A.1}$$

$$T_{t,0}^{Ocean} = T_{t-1,0}^{Ocean} + \frac{\Delta t}{C_{Ocean}} \left[\Delta Q_t - \frac{1-f}{\lambda_0} T_{t-1,0}^{Ocean} + \frac{A_{Land}}{1-A_{Land}} \nu \left(T_{t-1}^{Land} - T_{t-1,0}^{Ocean} \right) \right. $$
$$\left. + \kappa \frac{T_{t-1,1}^{Ocean} - T_{t-1,0}^{Ocean}}{\Delta z} \right], \tag{A.2}$$

$$T_{t,z}^{Ocean} = T_{t-1,z}^{Ocean} + \Delta t \left[\chi \frac{T_{t-1,z+1}^{Ocean} - 2T_{t-1,z}^{Ocean} + T_{t-1,z-1}^{Ocean}}{(\Delta z)^2} - w \frac{T_{t-1,z}^{Ocean} - T_{t-1,z-1}^{Ocean}}{\Delta z} \right] \quad \forall z \in [1,D), \tag{A.3}$$

and

$$T_{t,D}^{Ocean} = T_{t-1,D}^{Ocean} - \Delta t w \frac{T_{t-1,0}^{Ocean} - T_{t-1,D}^{Ocean}}{D}, \tag{A.4}$$

where Δt represents the discrete time step and Δz is the vertical distance of the discrete ocean layers used in the solution.

B Initialization of Climate Models

One important step in operationalizing these simple climate models is the process of initialization. Part of this process entails setting up each run of the model to ensure that it satisfies hard constraints in the form of currently observed anomalies given the assumed equilibrium climate sensitivity. Following Andreae et al. (2005) and Kiehl (2007) we derive the current level of additional forcing by balancing earth's theoretical energy budget. Specifically, the forcing of the climate system, ΔQ_t [W/m^2], must be equal to the energy escaping to space, $\lambda \Delta T_t$ [W/m^2], and the energy stored in the oceans, H_t [W/m^2], such that

$$\Delta Q_t = \frac{1}{\lambda} \Delta T_t + H_t. \tag{B.1}$$

The parameter λ [C m^2/W] represents the strength of the climate response and associated feedbacks and may be interpreted as in Section 2, such that $\lambda = \lambda_o/(1-f)$ and

$$\Delta Q_t = \frac{1-f}{\lambda_0} \Delta T_t + H_t. \tag{B.2}$$

We tie down our historical path of radiative forcing in the year 2000 and following Wigley (2005) assume anomalies of $\Delta T_{2000} = 0.7$ C and $H_{2000} = 0.7$ W/m^2, such that (B.2) may be rewritten as

$$\Delta Q_{2000} = 2.89 - 2.19f. \tag{B.3}$$

Given the assumption of Section 2.1 that $f \sim (0.61, 0.017^2)$, this would imply a median value of $\Delta Q_{2000} = 1.6$ W/m^2 which is in line with the 2000-2005 average estimate of 1.6 W/m^2 presented in the fourth assessment report of the IPCC (2007). It is worth noting that the relationship in (B.3) states that in cases of stronger (weaker) climate feedbacks the forcing required to produce the currently observed anomalies must be lower (higher). If one were to ignore this relationship and assume known forcing when integrating over the uncertain climate feedback parameter, as is commonly done within the suite of IAMs studied in this paper, the tails of the projected temperature response will be artificially extended.

When running Monte Carlo simulations to integrate over the uncertain feedback parameter we use (B.3) to define the year 2000 forcing for each draw of f. This value is then used to calibrate a piecewise linear function representing the historical path of radiative forcing used to initialize the internal variables of each climate model. The piecewise linear path of radiative forcing uses two breakpoints in the years 1900 and 1960 where the amount of forcing is defined as $\pi_{1900}\Delta Q_{2000}$ and $\pi_{1960}\Delta Q_{2000}$, respectively. The radiative forcing from 1800 to 2000 is then defined as

$$Q_t = \begin{cases} \Delta Q_{2000} \frac{(t-1800)\pi_{1900}}{100} & \text{if } t < 1900 \\ \Delta Q_{2000} \left[\pi_{1900} + \frac{(t-1900)(\pi_{1960}-\pi_{1900})}{50} \right] & \text{if } 1900 \leq t < 1960 \\ \Delta Q_{2000} \left[1 - \frac{(2000-t)(1-\pi_{1960})}{50} \right] & \text{if } 1960 \leq t < 2000 \end{cases} \quad . \tag{B.4}$$

We use values of $\pi_{1900} = 0.10$ and $\pi_{1960} = 0.30$ to match the relationship found in the historical path of radiative forcing as projected by MAGICC version 5.3 using its default set of assumptions regarding historical emissions. These values also lead to a path of radiative forcing similar to Figure 2.23 in the fourth assessment report of the IPCC (2007).

Past the year 2000 radiative forcing is defined as ΔQ_{2000} plus the additional forcing projected along the MiniCAM EMF-22 emissions scenario extended to 2300 as discussed in Section 4.2. Specifically we use the MAGICC version 5.3 and its default assumptions about historical emissions and atmospheric gas cycles to derive the additional radiative forcing given the emissions scenario from 2000 to 2300. The resulting baseline path of radiative forcing is presented in Figure B.1. The shaded are is the 95% confidence interval and the solid line represents the mean.

References

Andreae, M., Jones, C., and Cox, P. (2005). Strong present-day aerosol cooling implies a hot future. *Nature*, 435(7046): 1187–1190. ISSN 0028-0836.

Anthoff, D., and Tol, R. (2010). The CLimate Framework for Uncertainty, Negotiation, and Distribution (FUND), Technical Description, Version 3.5.

Armour, K., and Roe, G. (2011). Climate commitment in an uncertain world. *Geophysical Research Letters*, 38(1): L01707. ISSN 0094-8276.

Baker, M., and Roe, G. (2009). The shape of things to come: why is climate change so predictable? *Journal of Climate*, 22(17): 4574–4589. ISSN 1520-0442.
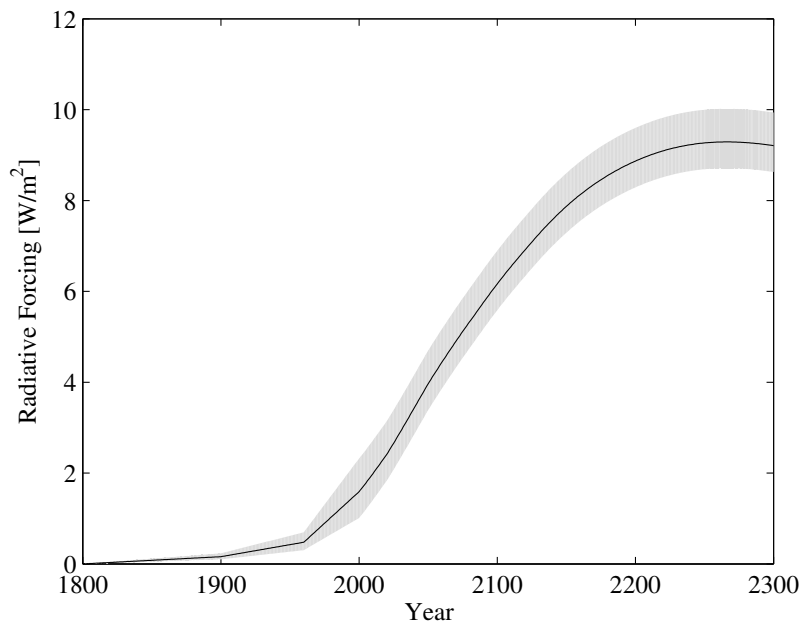
Figure B.1: Radiative Forcing Scenario

Bony, S., Colman, R., Kattsov, V., Allan, R., Bretherton, C., Dufresne, J., Hall, A., Hallegatte, S., Holland, M., Ingram, W., et al. (2006). How well do we understand and evaluate climate change feedback processes? *Journal of Climate*, 19(15): 3445–3482.

Calvin, K., Edmonds, J., Bond-Lamberty, B., Clarke, L., Kim, S., Kyle, P., Smith, S., Thomson, A., and Wise, M. (2009). 2.6: Limiting climate change to 450 ppm CO2 equivalent in the 21st century. *Energy Economics*.

Hansen, J., Lacis, A., Rind, D., Russell, G., Stone, P., Fung, I., Ruedy, R., and Lerner, J. (1984). *Climate Sensitivity: Analysis of Feedback Mechanisms*. Amer Geophysical Union. ISBN 0875904041.

Hansen, J., Russell, G., Lacis, A., Fung, I., Rind, D., and Stone, P. (1985). Climate response times: dependence on climate sensitivity and ocean mixing. *Science*, 229(4716): 857. ISSN 0036-8075.

Hansen, J., Sato, M., Kharecha, P., Beerling, D., Berner, R., Masson-Delmotte, V., Pagani, M., Raymo, M., Royer, D., and Zachos, J. (2008). Target Atmospheric CO2: Where Should Humanity Aim? *Open Atmospheric Science Journal*, 2: 217–231.

Hoffert, M., Callegari, A., and Hsieh, C. (1980). The role of deep sea heat storage in the secular response to climatic forcing. *Journal of Geophysical Research*, 85(C11): 6667–6679. ISSN 0148-0227.

Hope, C. (2006). The marginal impact of CO2 from PAGE2002: An integrated assessment model incorporating the IPCC's five reasons for concern. *Integrated Assessment*, 6(1).

Hope, C. (2008). Optimal carbon emissions and the social cost of carbon over time under uncertainty. *Integrated Assessment*, 8(1). ISSN 1389-5176.

IPCC (2007). Contribution of Working Group I to the Fourth Assessment Report to the Intergovernmental Panel on Climate Change. In *Physical Science Basis*. Cambridge University Press.

Kattenberg, A., Giorgi, F., Grassl, H., Meehl, G., Mitchell, J., Stouffer, R., Tokioka, T., Weaver, A., Wigley, T., et al. (1996). Climate models - projections of future climate. *Climate change 1995: The science of climate change*, pages 285–357.

Kiehl, J. (2007). Twentieth century climate model response and climate sensitivity. *Geophysical Research Letters*, 34(22): L22710. ISSN 0094-8276.

Knutti, R., and Hegerl, G. (2008). The equilibrium sensitivity of the Earth's temperature to radiation changes. *Nature Geoscience*, 1(11): 735–743. ISSN 1752-0894.

Lindzen, R., and Giannitsis, C. (1998). On the climatic implications of volcanic cooling. *Journal of Geophysical Research*, 103(D6): 5929–41.

Marten, A., and Newbold, S. (2011). Estimating the Social Cost of Non-CO2 GHG Emissions: Methane and Nitrous Oxide. *NCEE Working Paper Series*.

Mitchell, J. (1989). The "greenhouse" effect and climate change. *Reviews of Geophysics*, 27(1): 115–139. ISSN 8755-1209.

Morgan, M., and Dowlatabadi, H. (1996). Learning from integrated assessment of climate change. *Climatic Change*, 34(3): 337–368. ISSN 0165-0009.

Narita, D., Tol, R., and Anthoff, D. (2010). Economic costs of extratropical storms under climate change: an application of FUND. *Journal of Environmental Planning and Management*, 53(3): 371–384. ISSN 0964-0568.

Newbold, S., and Daigneault, A. (2009). Climate response uncertainty and the benefits of greenhouse gas emissions reductions. *Environmental and Resource Economics*, 44(3): 351–377. ISSN 0924-6460.

Nordhaus, W. (1993). Optimal greenhouse-gas reductions and tax policy in the" DICE" model. *The American Economic Review*, 83(2): 313–317.

Nordhaus, W. (2007a). The Challenge of Global Warming: Economic Models and Environmental Policy. *New Haven, CT: Yale University*.

Nordhaus, W. (2007b). Two centuries of productivity growth in computing. *The Journal of Economic History*, 67(01): 128–159. ISSN 0022-0507.

Nordhaus, W. (2010). Economic aspects of global warming in a post-Copenhagen environment. *Proceedings of the National Academy of Sciences*, 107(26): 11721. ISSN 0027-8424.

Nordhaus, W., and Boyer, J. (2000). *Warming the world: economic models of global warming*. The MIT Press.

Plambeck, E., and Hope, C. (1996). PAGE95. An updated valuation of the impacts of global warming. *Energy Policy*, 24(9): 783–793.

Ramsey, F. (1928). A mathematical theory of saving. *The Economic Journal*, 38(152): 543–559.

Roe, G. (2009). Feedbacks, timescales, and seeing red. *Annual Review of Earth and Planetary Sciences*, 37: 93–115.

Roe, G., and Baker, M. (2007). Why is climate sensitivity so unpredictable? *Science*, 318(5850): 629.

Shine, K., Fuglestvedt, J., Hailemariam, K., and Stuber, N. (2005). Alternatives to the global warming potential for comparing climate impacts of emissions of greenhouse gases. *Climatic Change*, 68(3): 281–302.

Stern, N. (2006). *Stern Review: The economics of climate change*, volume 30. Cambridge University Press.

Tol, R. (1997). On the optimal control of carbon dioxide emissions: an application of FUND. *Environmental Modeling and Assessment*, 2(3): 151–163. ISSN 1420-2026.

USG (2010). Technical Support Document: Social Cost of Carbon for Regulatory Impact Analysis Under Executive Order 12866.

van Vuuren, D., Lowe, J., Stehfest, E., Gohar, L., Hof, A., Hope, C., Warren, R., Meinshausen, M., and Plattner, G. (2009). How well do integrated assessment models simulate climate change? *Climatic Change*, pages 1–31. ISSN 0165-0009.

Warren, R., Mastrandrea, M., Hope, C., and Hof, A. (2010). Variation in the climatic response to SRES emissions scenarios in integrated assessment models. *Climatic change*, pages 1–15. ISSN 0165-0009.

Weitzman, M. (2009). On modeling and interpreting the economics of catastrophic climate change. *The Review of Economics and Statistics*, 91(1): 1–19. ISSN 0034-6535.

Weitzman, M. (2010). GHG targets as insurance against catastrophic climate damages. *NBER Working Paper*.

Wigley, T. (2005). The climate change commitment. *Science*, 307(5716): 1766.

Wigley, T., and Raper, S. (1992). Implications for climate and sea level of revised IPCC emissions scenarios. *Nature*, 357: 293–300.

Please note:

You are most sincerely encouraged to participate in the open assessment of this discussion paper. You can do so by either recommending the paper or by posting your comments.

Please go to:

The Editor